Integrated operational monitoring and fault early warning system for wheat combine harvesters based on CAN bus

Weipeng Zhang, Hongze Guo, Bo Zhao*, Suchun Liu, Liming Zhou,
Fengzhu Wang, Zongbin Li, Yangchun Liu
(*State Key Laboratory of Agricultural Equipment Technology, Chinese Academy of Agricultural Mechanization Sciences Group Co., Ltd., Beijing 100083, China*)

Abstract: The core objective of this study is to address critical challenges in the operational monitoring and fault early warning of wheat combine harvesters. To this end, this study designed a field-oriented multi-parameter detection system for wheat combine harvesters, which utilizes the CAN bus and virtual instrumentation. Key challenges in this field include three aspects: first, manual inspection is inefficient and lacks automated detection methods, making it difficult to meet the real-time requirements of large-scale operations; second, fault early warning accuracy is low, as single-parameter evaluation is prone to false positives and false negatives; third, monitoring parameters function in isolation, leading to significant data inconsistencies that hinder the early detection of potential faults. To address these issues, this study focuses on three key tasks: establishing a multi-parameter collaborative monitoring framework, optimizing hardware and communication protocols, and developing data processing methods for fault detection and warning. Specifically, sensors for fuel consumption, Hall-effect rotational speed, and strain-gauge torque are deployed at critical components of the harvester. The system then efficiently transmits operational status data via the CAN bus to a processing module, enabling remote real-time monitoring of the harvester’s comprehensive operational conditions. For the designed fault warning algorithm, it dynamically adjusts warning thresholds by comparing characteristic parameters with historical data, thereby achieving accurate fault identification and timely warning responses. This study innovatively transmitted multi-source sensor data through the high-anti-interference CAN bus and developed a fault warning algorithm incorporating feature recognition and dynamic thresholds. In simulated experiments, the measurement errors of both instantaneous and cumulative fuel consumption were ≤5%, while the system achieved a warning accuracy of 97.3% and a response time of ≤180 ms. This represents a 15.3-percentage-point improvement in accuracy compared to traditional single-parameter warning systems. Overall, this study addresses the challenge of multi-parameter integrated monitoring for wheat combine harvesters and provides a scalable technical solution for hardware integration and comprehensive data analysis. It also offers a reference for the intelligent upgrading of Chinese harvesters, which is expected to accelerate the transformation of agricultural mechanization toward precision and informatization.

Keywords: combine harvester, comprehensive monitoring, fault early warning, CAN bus, visualization system
DOI: 10.25165/j.ijabe.20261901.8941

Citation: Zhang W P, Guo H Z, Zhao B, Liu S C, Zhou L M, Wang F Z, et al. Integrated operational monitoring and fault early warning system for wheat combine harvesters based on CAN bus. Int J Agric & Biol Eng, 2026; 19(1): 170–178.

1 Introduction

In the course of agricultural modernization, precision farming has placed increasing demands on the intelligence and informatization of agricultural machinery. As critical equipment for grain production, the operational parameter monitoring and working condition control capabilities of combine harvesters directly determine operational efficiency and harvest quality[1-3].

Currently, significant disparities exist in the development of monitoring technologies for rice and wheat combine harvesters both domestically and internationally, with both facing bottlenecks requiring urgent breakthroughs[4]. Internationally, companies such as John Deere in the United States and Massey Ferguson under AGCO have developed grain combine fault monitoring systems capable of real-time monitoring of basic combine parameters[5-9]. However, their technological systems are closed, with limited compatibility in core protocols and hardware, coupled with high equipment costs, making them difficult to adapt and promote on domestic small and medium-sized harvesting machinery[10-14]. Current domestic research primarily monitors isolated or limited machine parameters, with relatively independent monitoring data lacking comprehensive operational status integration. This prevents correlation analysis[15-17], resulting in low fault warning accuracy that fails to meet precision agriculture’s demand for refined operational process control.

To address the aforementioned issues, this study proposes a bus-based multi-source parameter integration monitoring system design for wheat combine harvesters. Its core innovations are reflected in three aspects: First, establishing a multi-parameter collaborative monitoring system. By correlating operational parameters such as

---

Received date: 2024-03-21 **Accepted date:** 2025-11-17

Biographies: Weipeng Zhang, Engineer, research interest: agricultural machinery collaboration, Email: zhangwellp@163.com; **Hongze Guo**, Master candidate, research interest: automatic agricultural machinery, Email: johnguohz@163.com; **Suchun Liu**, PhD candidate, research interest: fruit harvesting robot, Email: suchun1804@163.com; **Liming Zhou**, Researcher, research interest: intelligent control of agricultural machinery, Email: haibo1129@163.com; **Fengzhu Wang**, Senior engineer, research interest: intelligent measurement and control of agricultural machinery, Email: wangfengzhu1@126.com; **Zongbin Li**, Master candidate, research interest: intelligent agricultural machinery, Email: 1307791409@qq.com; **Yangchun Liu**, Researcher, research interest: agricultural equipment measurement and control, Email: lyc215@163.com.

***Corresponding author: Bo Zhao**, Researcher, research interest: agricultural robot. Chinese Academy of Agricultural Mechanization Sciences Group Co., Ltd., Beijing 100083, China. Email: zhaoboshi@126.com.

engine speed, mileage, feed rate, grain loss rate, and moisture content, it achieves a comprehensive evaluation of overall machine performance, overcoming the limitations of traditional single-parameter monitoring[18]. Second, a standardized CAN bus communication architecture ensures efficient transmission of operational parameters, maintaining packet loss below 0.5% and transmission latency under 50 ms, thereby enhancing system compatibility and reliability. Third, the intelligent data analysis module incorporates a dynamic threshold adjustment algorithm, enabling fault prediction through comparison of historical data with real-time parameters[19-21]. Integrated data storage and visualization capabilities support operational process review and parameter trend analysis, providing data-driven support for precise operational optimization.

Through innovative design encompassing hardware integration, standardized communication protocols, and collaborative data analysis[22,23], this system effectively addresses the fragmentation and low precision issues plaguing existing monitoring systems[24,25]. It simultaneously circumvents the closed-system nature and high-cost drawbacks of foreign technologies, offering a scalable technical solution for the intelligent upgrading of wheat combine harvesters. This facilitates the deep implementation of precision agriculture technologies within field operation scenarios.

2 System architecture

2.1 Module interconnection and data flow

Wheat combine harvesters face three core environmental challenges during field operations: intense electromagnetic interference, severe vibration, and fluctuating levels of dust and humidity. The intrinsic characteristics of the CAN communication module are well-suited to address these issues. Specifically, its high transmission speed and ability to interface with multiple peripheral modules facilitate real-time data transmission. In this design, the CAN bus serves as the system's core backbone, connecting the perception, control, and execution modules—including multiple sensors, on-board terminals, and actuators.

Figure 1 illustrates the overall architecture of the online monitoring system for wheat combine harvester operational status. Key monitoring parameters are categorized into three groups: first, machine status indicators such as component rotational speed and torque; second, operational quality metrics including crushing rate, impurity content, and loss rate; and third, operational status data encompassing travel speed, positioning information, header height, and grain flow rate. The monitoring system primarily consists of an onboard monitoring terminal, a CAN communication module, a torque sensor, a torque acquisition and control unit, a motor speed sensor, and a BeiDou positioning module. The torque sensor, torque acquisition and control unit, and motor speed sensor communicate via the CAN bus. This bus supports integration with multiple expandable sensors, enabling real-time transmission of monitoring data such as rotational speed and torque. As the system's data processing hub, the onboard monitoring terminal performs three core functions: receiving and processing data from all modules, issuing control commands, and supporting human-machine interaction. Additionally, it connects to the BeiDou positioning module via a serial port to acquire and upload the harvester's real-time location and travel speed data.

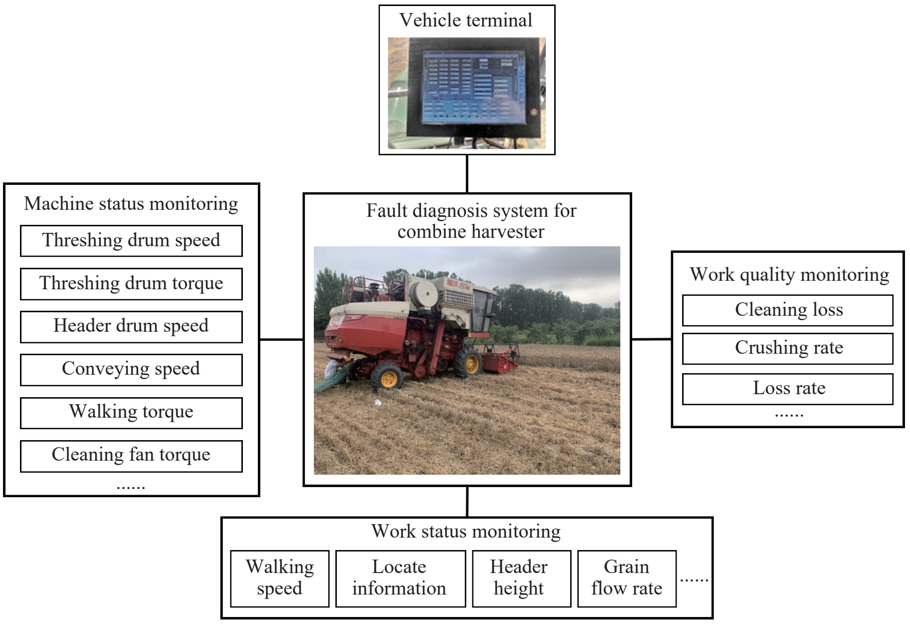

Figure 1 Composition of the combine harvester working condition monitoring system

During the operation of agricultural machinery, remote monitoring systems facilitate core functions such as positioning and operational status monitoring. In the event of faults during operation, alerts are transmitted to the remote terminal, which then verifies the fault details and triggers a corresponding response. The Lovol Gushen GE60 (4LZ-6E3) wheat combine harvester was used as the test platform for this system, with its key parameters presented in Table 1. The design of the system modules was fully tailored to the mechanical structure and operational parameter range of this specific model. To ensure stable data acquisition, the installation locations of the sensors were selected to avoid regions with intense vibration.

2.2 Hardware architecture design

The hardware architecture of the wheat combine harvester monitoring system adopts a three-tier structure, which includes sensor data acquisition, communication transmission, and on-board terminal control. This architecture is shown in Figure 2. Specifically, torque sensors monitor the feed intake, flow sensors track the grain throughput, grain loss sensors measure the total grain loss rate, radar ground speed sensors monitor the travel speed, optical encoders capture the rotational speeds of the threshing drum and grain conveyor auger, and ultrasonic sensors enable real-time detection of the header height. Each sensor node serves as an independent CAN node to enable distributed parameter acquisition.

The on-board terminal layer integrates an ARM processor (S3C2410), flash memory, VGA interface, USB interface, CAN interface, and Ethernet interface to form the system's intelligent control terminal. The ARM processor S3C2410 interfaces with the CAN bus via a CAN controller to transmit and receive data. Meanwhile, it connects to a monitor through the VGA interface to display all operational parameters.

Table 1 Main parameters of Lovol GE60 (4LZ-6E3) harvester

Performance indicators	Technical parameters
Dimensions/(mm×mm×mm)	6600×3000×3420
Header width/mm	2510
Feed volume/kg·s^{-1}	0-6
Speed/km·h^{-1}	2-4
Rated power/kW	107
Minimum ground clearance/mm	350
Drive wheel tread/mm	2060
Work efficiency/hm^2·h^{-1}	0.3-1.2

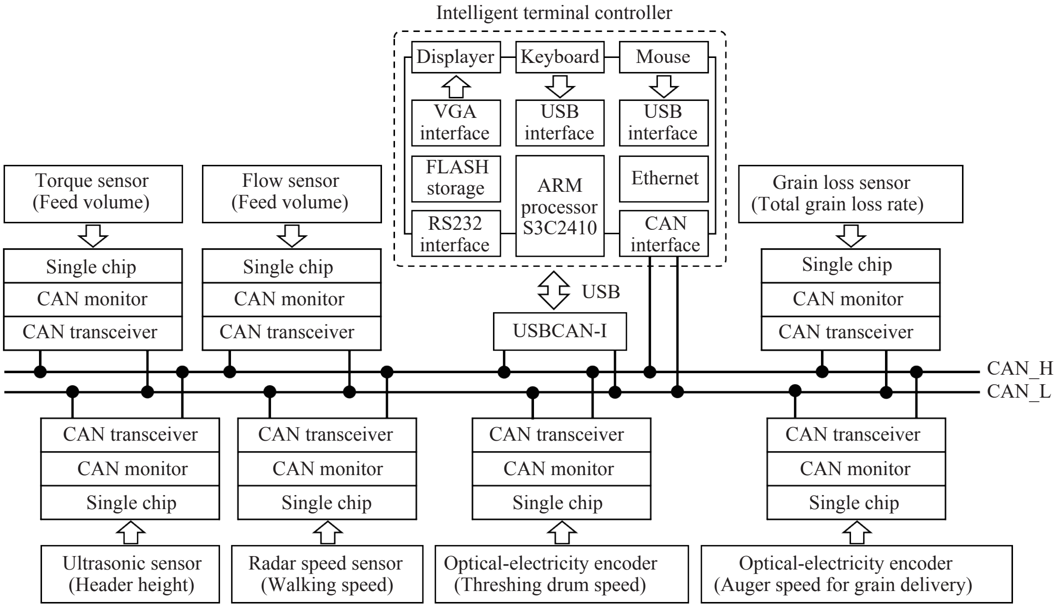

Figure 2 Hardware structure diagram

During field operations, the crop feed rate of a combine harvester fluctuates continuously due to factors including grain flow rate, harvester forward speed, and header height. The operational status of the combine harvester is closely correlated with its forward speed, feed rate, threshing drum rotational speed, grain conveyor auger speed, and total grain loss rate. Therefore, parameters such as the harvester's forward speed can be adjusted to maintain a reasonable and uniform feed rate - thereby stabilizing the load on the threshing drum and grain conveyor auger, and ensuring that the harvester's total loss rate does not exceed preset permissible limits. The communication transmission layer in the system's hardware exchanges signals with the controller via the CAN bus. Specifically, it transmits the current status signals collected by the sensors to the microcontroller. After receiving and processing these signals, the microcontroller outputs corresponding commands to the actuators to adjust the harvester's operating parameters.

2.3 Software architecture and hardware-software synergy

The software architecture design is centered on stability, reliability, real-time performance, and flexible scalability. It adapts to the characteristics of hardware-based distributed acquisition and centralized control, adhering to the following three design principles:

First is the principle of modular fault-tolerant design. Software is divided into multiple independent modules based on specific hardware functions. Each submodule is compiled and tested independently, enabling replacement of faulty components without affecting overall system operation. When abnormal data occurs, the system automatically replaces it with the latest valid data stored in flash memory, thereby preventing system crashes caused by data anomalies.

Second is the real-time assurance design principle. The real-time operating system prioritizes tasks based on criticality. Core tasks, such as abnormal feed rate response and fault alarms, are assigned the highest priority, while non-real-time tasks like data storage receive lower priority. Upon receiving warning information, the system can immediately issue control commands to prevent potential failures.

Finally, the design principles of scalability and compatibility. Standardized interfaces are adopted, eliminating the need for additional protocol conversion modules when integrating new devices. Additionally, modifying parameters does not require software recompilation, enabling plug-and-play functionality.

The system employs a mechanism in which software and hardware modules operate independently with clearly delineated functions. Meanwhile, software and hardware interact through an integrated collaborative model. This enables real-time monitoring and adaptive control of the wheat harvester's operating parameters through a closed-loop process involving data exchange and status feedback.

3 Key parameter monitoring

3.1 Engine fuel consumption monitoring

Engine fuel consumption is the most critical indicator for evaluating an engine's economic performance, operational cost-effectiveness, and energy-saving and emission-reduction performance. For combine harvesters, it also serves as a key metric for assessing reliability and comprehensive operational performance. Consequently, the accurate measurement of fuel consumption is of great significance and practical value for understanding the operational status of combine harvesters, as well as for fault early warning and diagnosis.

As shown in Figure 3, the monitoring device for measuring fuel consumption in combine harvester engines is installed between the fuel tank and the fuel pump. Its operating principle is as follows: Fuel flows unidirectionally through the supply line, passes through the flow meter, and is supplied to the engine. Simultaneously, fuel returning via the return line flows into the return chamber. When the return chamber fills with fuel, it activates the integrated ball-rod mechanism of the float switch, thereby opening the solenoid valve and energizing the switch. At this point, the return fuel is directly injected into the engine.

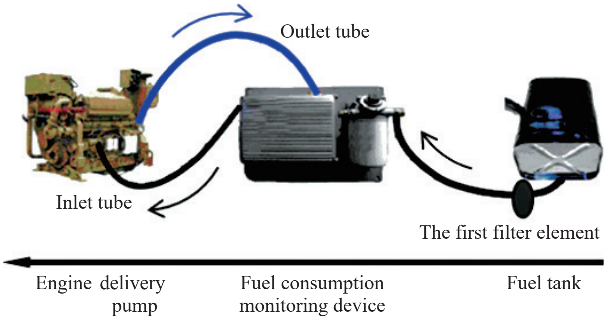

Figure 3 Structure diagram of real-time fuel consumption monitoring system

Among the available options, a mass flow meter was selected for its capability to directly measure fuel consumption based on fluid mass. This selection avoids the effects of diesel temperature and density variations on measurement accuracy. The chosen flow sensor, model CMFS100M, measures mass flow rates ranging from 0.05 to 50.00 kg/h and volumetric flow rates from 0.06 to 60.00 L/h - encompassing the harvester’s entire operating range, from idle (low flow) to full load (high flow). With an accuracy class of ±0.10% FS, it exceeds industry standards for fuel consumption measurement in agricultural machinery, thereby ensuring the reliability of both instantaneous and cumulative fuel consumption data.

Figure 4 shows the actual installation layout of the real-time fuel consumption monitoring system on the Lovol Gushen GE60 (4LZ-6E3) wheat combine harvester. Considering the harvester’s structural constraints and space limitations, the system is mounted in the lower right section of the cab to avoid proximity to the engine’s high-temperature zone, preventing overheating from affecting the flow meter’s accuracy. Its position adjacent to the onboard terminal minimizes CAN bus cable length, thereby reducing signal attenuation.

To verify the system’s measurement accuracy, the Lovol Gushen GE60 (4LZ-6E3) wheat combine harvester, equipped with the real-time fuel consumption monitoring system, was used as the experimental vehicle. Four typical wheat harvesting scenarios were simulated by adjusting the forward speed and cutting width to control the feed rate. For each operating condition, after the engine stabilized, the monitoring device collected fuel consumption data within the designated measurement period. Meanwhile, a high-precision volumetric fuel meter was used as the reference instrument to record cumulative fuel consumption. After the test, the measurement deviation between the two devices was calculated. Each operating condition was measured three times, and the arithmetic mean was taken as the final result.

Field trial data, as listed in Table 2, indicate that under typical operating conditions (no load, light load, full load, and overload), both the instantaneous fuel consumption rate and cumulative fuel consumption exhibit measurement errors within 5%. This validates the strong functional adaptability and high measurement precision of the fuel consumption monitoring device, meeting the design objectives. Compared to traditional manual weighing methods, the device significantly improves the efficiency of internal combustion engine fuel consumption testing. It provides an efficient and reliable measurement tool for optimizing the fuel economy of wheat combine harvesters and calculating their operational costs.

Figure 4 Installation diagram of real-time fuel consumption monitoring

Table 2 Fuel consumption error under different operating conditions

Test conditions	Running speed/ $km\cdot h^{-1}$	Feed rate/ $kg\cdot s^{-1}$	Reference measurement value/L	Device measurement value/L	Absolute error/L	Relative error/%
No load	4.0	0	3.82	4.02	+0.21	4.6
Light load	2.5	1.8	7.56	7.48	+0.24	4.2
Fully loaded	3.0	4.2	15.32	14.98	+0.53	3.9
Overload	2.0	6.5	21.48	23.11	+1.02	4.9

3.2 Monitoring of working component rotational speed

During combine harvester operation, forward speed is primarily influenced by field conditions, grain moisture content, and terrain. Excessive speed may result in crop loss, while insufficient speed increases grain feed rate, potentially causing threshing drum blockages. Monitoring critical working components is essential for ensuring the reliable operation of all parts. To meet the need for monitoring the actual operating speed of the combine harvester, this study implemented monitoring on the auger, fan, conveyor belt, threshing drum, and positioning system. As shown in Figure 5, rotational speed monitoring involves collecting seven speed signals: header speed, streamline cutting drum speed, fan speed, conveyor belt speed, elevator auger speed, straw auger speed, and grain auger speed.

This system employs non-contact sensors manufactured by Danfoss for measurement. These sensors avoid direct friction with rotating components, thereby extending their service life. They integrate Hall-effect speed measurement devices, specifically the MBS 1250 model, designed for the harsh operating environments of agricultural machinery. This model withstands the dusty conditions and high vibration encountered during combine harvester operations. It provides standard CAN signal output compliant with the SAE J1939 protocol, eliminating the need for additional protocol conversion modules. The MBS 1250 measures rotational speeds from −2500 to 2500 r/min, covering all rotating components: threshing drum 600-800 r/min, fan 800-1200 r/min, etc. With an accuracy of ±0.1% FS, this sensor precisely detects motor rotation direction and speed.

To meet rotational speed testing requirements, Hall Effect sensors were installed at eight rotating shaft positions on the test combine harvester: the cutter bar, feed auger, conveyor auger, threshing drum, fan, straw walker, vibrating sieve, and grain auger. This setup allows for real-time acquisition of motor speed data from key working mechanisms. The field installation of these critical speed sensors is shown in Figure 6.

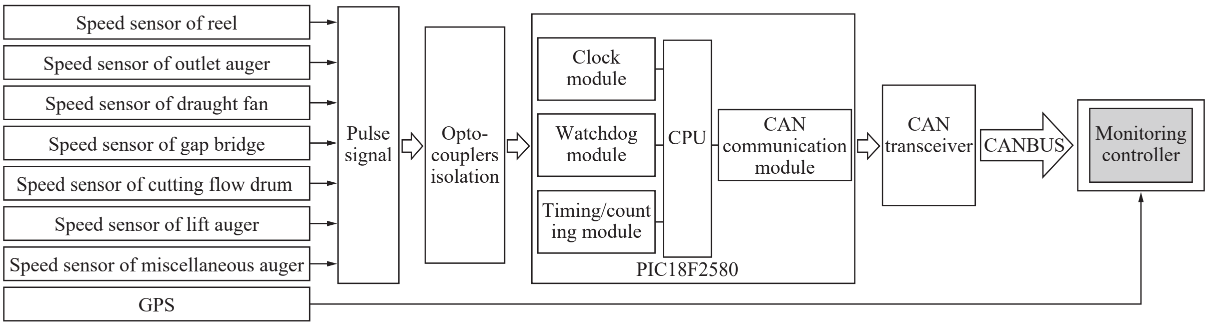

Figure 5 Schematic diagram of speed monitoring for key working components

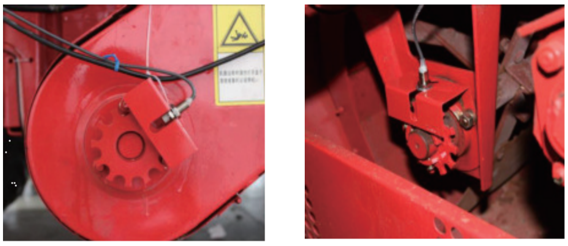

a. Increase the speed monitoring of the auger

b. Fan speed monitoring

c. Header auger speed monitoring

d. Shearing drum speed monitoring

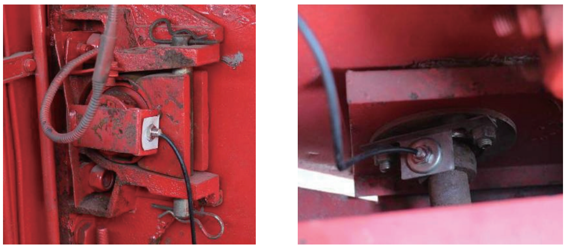

e. Bridge speed monitoring

f. Residual agitator speed monitoring

Figure 6 Speed sensor installation diagram

3.3 Torque monitoring of critical components

3.3.1 Torque acquisition controller

Figure 7 illustrates the schematic architecture of a torque acquisition controller based on the Microchip PIC18F2580 microprocessor. This high-performance 8-bit microcontroller features a comprehensive peripheral suite, including two enhanced USART modules, one CAN module, one MSSC module, an 8-channel 12-bit ADC module, five 8/16-bit timer/counter modules, and five CCP/ECCP modules. The core strengths of the entire system lie in its low power consumption, high-speed operation, powerful functionality, and strong anti-interference capabilities, making it particularly suitable for automation scenarios demanding low power, high reliability, and high efficiency. Additionally, the digital signal isolation module integrates bus fault protection functionality. When a bus short circuit is detected, the module automatically enters a high-impedance state, thereby preventing adverse effects on other nodes within the network.

The MCU’s CAN module employs the TJA1050 CAN transceiver, which converts the MCU’s output signals into CAN bus differential signals for transmission to the CAN bus network. This enables the MCU to function as a signal bridge between the torque sensor and the system’s CAN bus, performing five core functions: torque signal reception, pre-processing, ADC conversion, CAN protocol encapsulation, and fault diagnosis. This setup fulfills the torque monitoring requirements of critical components in wheat combine harvesters, such as the threshing drum and drive shaft.

3.3.2 Signal conditioning and conversion

The torque-speed sensor is powered in a non-contact manner via a set of toroidal transformers mounted on the sensor. Torque signals are received by the sensor and transmitted to the input interface of the controller. The controller employs strain gauge bridge electrical measurement technology: the weak torque signals detected by the strain gauge bridge first undergo differential amplification. Subsequently, high-frequency noise is filtered out through a filter, and a voltage regulator diode is used to stabilize the signal, ensuring stable transmission to the CCP module. After voltage-to-frequency conversion, a frequency signal proportional to the measured torque is output in a non-contact manner via a low-power signal coupler.

Under no-load conditions, the designed torque monitoring sensor outputs a 10 kHz frequency signal. During forward rotation at full load, it outputs 15 kHz; during reverse rotation at full load, it outputs 5 kHz. The sensor achieves a full-scale measurement accuracy of ±0.5%.

The torque measurement device also integrates a Hall-effect speed sensor. By using the rotational speed data transmitted by this sensor, the operating power of rotating components can be calculated, providing a basis for subsequent overload protection. Within the system, the operating torque of each rotating component is estimated based on the drive power of the wheat combine harvester, thereby determining the measurement range of the torque sensor as 0-1000 N·m.

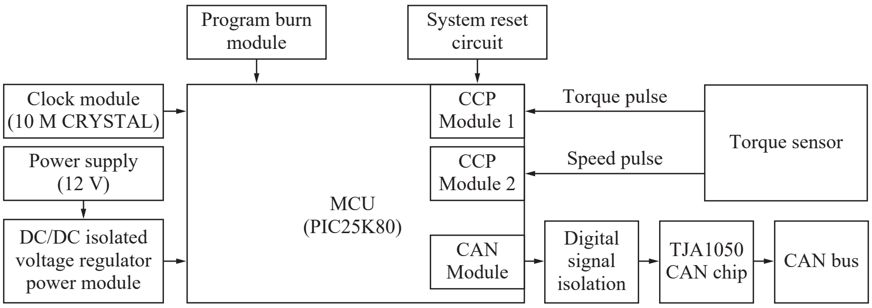

Figure 7 Schematic diagram of torque acquisition controller

3.3.3 Installation of torque sensors

Figure 8a shows the installation of sensors on the shredding rollers and discharge fan. A replaceable pulley-type torque sensor is employed, which requires no modification to the shaft structure. This involves fabricating a drive pulley from a material with desirable elastic modulus properties to replace the original pulley. Torque strain gauges are attached to measure the elastic deformation of the drive pulley, thereby indirectly deriving the torque of the measured shaft. During operation, the pulley first drives the inner rotating shaft of the torque sensor; the outer rotating shaft of the sensor then transmits power back to the load shaft. In this way, the strain bridge affixed to the torque sensor shaft can indirectly acquire load information from the measured shaft.

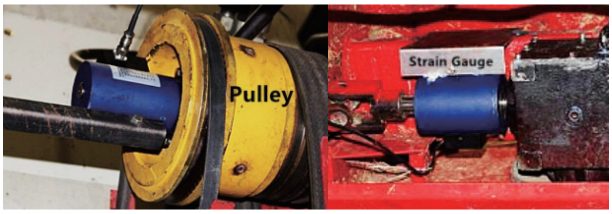

a. Fan torque sensor monitoring

b. Traveling transmission shaft torque sensor installation

Figure 8 Installation diagram of the torque sensor

Figure 8b shows the field installation of sensors on the travel shaft and cutting platform. A strain gauge torque sensor is mounted on the shaft, with the strain gauges positioned vertically during installation. This configuration eliminates static strain induced by the self-weight of the shaft system, thereby improving measurement accuracy.

3.3.4 Lead wire specifications and precision control

All lead wires use waterproof shielded cables with a certain degree of tensile elasticity. The power supply connectors adopt IP68 waterproof connectors, and waterproof tape is wrapped around the interfaces. During fixation, high-temperature or moving components are avoided; the wires are secured with cable ties between the harvester body and the iron frame. A 100 mm redundant length is reserved at the sensor end, arranged in a U-shaped bend to prevent lead wires from being stretched and broken due to harvester vibration.

The optimal installation angle for the Hall-effect speed sensor is such that the angle between the probe axis and the tangential direction of the gear disc's tooth tip is 0°, at which the magnetic flux change rate induced by the Hall element is maximized. Excessively large installation spacing leads to signal attenuation, while excessively small spacing causes probe wear; the optimal spacing is 1.0±0.2 mm, where the Hall element operates at the optimal sensing distance.

For the strain gauge torque sensor, the optimal installation angle requires the strain gauges to be bonded at 45° and 135° relative to the axial direction of the shafting, maximizing the strain value. The optimal coaxiality is defined as the coaxiality between the sensor's inner ring and the drive shaft being $\leq$0.03 mm, resulting in a radial runout of $\leq$0.05 mm and a measurement error caused by additional bending moment of $\leq$0.1% FS.

Through the aforementioned sensor selection optimization and installation design, stable performance was maintained during actual field operations in June 2022 under various working conditions, including no-load, light-load, full-load, overload, low temperature, high temperature, and high dust levels.

4 Fault early warning system design

4.1 Fault feature extraction algorithm

Traditional wheat combine harvesters primarily rely on single-static-threshold fault warning systems, which suffer from limitations such as delayed warnings, high false alarm rates, and the inability to predict potential failures. To address these issues, this system innovatively extracts pre-failure precursor features from multi-source sensor data. For instance, when minor crop entanglement occurs in the threshing drum without causing complete blockage, the synchronous speed reduction of the auger fails to trigger the system. This occurs because the lack of multi-parameter correlation prevents the early warning signal from being recognized. By integrating a parameter trend analysis module into the algorithm, such scenarios can be identified as potential early-stage fault indicators, enabling precise detection of minor blockage events.

The algorithm further assigns different weights to multi-source features, prioritizing those that significantly influence fault occurrence. For instance, in scenarios where threshing drum faults are prone to jamming, the system automatically increases the weight of torque features. This enhances the model's sensitivity to torque anomalies, enabling early fault prediction and precise diagnostics.

Additionally, an expert fault diagnosis system has been developed to enable precise fault cause identification and intelligent maintenance plan generation. This system was built upon a decade of wheat harvester fault cases and maintenance data, summarizing common failures and corresponding solutions for critical systems such as engines, transmission systems, and working units. When anomalies are detected, the system updates its memory and integrates the abnormal data into the database to prevent recurrence of faults. For instance, when engine RPM fluctuates beyond ± 50 rpm, coolant temperature exceeds 95°C, and fuel consumption increases by >10%, this indicates carbon buildup in the engine, necessitating shutdown for cleaning. During maintenance, selecting a specific combine model prompts the system to retrieve the maintenance knowledge base and generate step-by-step solutions. For a drum blockage fault, the system outputs the following steps:

first, shut down the combine and disconnect the power source; second, open the drum access door; then, clear crop residue from inside the drum; next, inspect the drum speed sensor; finally, restart the combine and conduct a test run.

4.2 Dynamic threshold alert algorithm

The false alarm and missed detection rates in mechanical fault early warning tests require algorithm optimization. For example, when the moisture content of wheat abruptly surges, elevated grain resistance may trigger spurious high-load warnings. This issue can be mitigated through dynamic threshold adjustment: upon detecting elevated moisture levels, the algorithm automatically increases the drum torque warning threshold. Similarly, when minor crop entanglement occurs in the drum without complete blockage, the synchronous reduction in auger speed lacks correlation with other parameters. This leads the system to miss this precursor signal, thereby resulting in a false negative. This problem can be resolved by integrating a parameter trend analysis module into the algorithm. This module identifies such scenarios as latent early-stage malfunction indicators, enabling the detection of minor blockage events.

As demonstrated by the early warning test validation results in Table 3, the system has significantly enhanced the accuracy and reliability of mechanical early warnings through dynamic threshold algorithm optimization.

Table 3 Early warning testing for different fault types

Fault type	Number of tests	Correct count before algorithm optimization	False alarms/times	Underreporting/times	Correct count after algorithm optimization	False alarms/ times	Underreporting/ times
Threshing drum blockage	6	4	1 (Vibration/Speed reduction)	1 (Minor entanglement)	6	0	0
Engine power deficiency	5	3	1 (Low-load power fluctuations)	1 (Power gradually decreases)	5	0	0
Abnormal cutting height	4	3	0	1 (High-altitude slow drift)	4	0	0
Disturbance under normal operating conditions	20	-	3 (Moisture content/Vibration)	-	-	0	-
Total	45	10	5	3	15	0	0

4.3 Fault early warning field testing of complete machinery

The Lovol Gushen GE60 (4LZ-6E3) wheat combine harvester was selected as the test prototype. Equipped with this fault warning system, it underwent a five-day field harvesting trial in Yingshang County, Anhui Province, during June 2022, targeting the Wanmai 33 wheat variety. The field trial scenario is shown in Figure 9.

In this trial, monitoring parameters from various sensors of the combine harvester were collected continuously. When the harvester reached the designated stopping zone, it was shut down. Manually weighed material samples served as actual reference values to calibrate the readings of the grain flow sensor. This process determined the sensor's relative error and verified the system's accuracy in monitoring real-time operational parameters. Table 4 presents the status records of each monitoring point during the normal operation of the combine harvester, with a recording interval of 1 s. The status data measured from each monitoring point is displayed in real time online and stored on a cloud platform.

Figure 9 Field experiment scenarios

Table 4 Field test records

No.	Longitude/ (°)	Latitude/ (°)	Speed/ km·h^{-1}	Instantaneous fuel consumption/mL·s^{-1}	Tangential flow drum speed/r·min^{-1}	Fan speed/ r·min^{-1}	Lifting auger speed/r·min^{-1}	Miscellaneous auger speed/r·min^{-1}	Grain entrainment loss/grains
1	116.34 482	32.70 191	2.47	4.85	652.85	898.50	584.32	496.55	85
2	116.34 271	32.70 041	3.05	4.79	669.25	912.33	612.28	522.34	101
3	116.34 415	32.70 138	3.55	4.54	684.37	934.88	622.34	538.65	113
4	116.34 415	32.71 011	2.78	5.11	612.23	834.32	573.25	494.58	98
5	116.34 329	32.70 179	3.24	4.83	644.25	811.26	566.35	485.62	92

To validate the operational reliability and stability of the monitoring system, its hardware and software were installed, calibrated, and debugged at designated locations on the test combine harvester. Operational testing was conducted in phases. Following installation and debugging, field trial preparations for the combine harvester commenced immediately to verify system feasibility and reliability. During testing, frequent blockages in the threshing chamber caused by varying crop conditions led to machine shutdowns and interrupted normal operations. Per safety requirements stipulated in the Lovol Gushen Combine Harvester Factory Technical Manual, if the threshing drum speed falls below 80% of the rated speed, the equipment must immediately cease operation for maintenance. To this end, the monitoring system automatically triggers an audible alarm to alert the operator. Once the speed of the internal threshing components returns to normal, the system emits another audible signal indicating the operator can resume work, thereby achieving fault prediction. Table 5 lists the fault alarm test results, demonstrating an accuracy rate exceeding 95% across all scenarios, fully showcasing the system's outstanding early warning performance.

4.4 Cloud platform data processing and storage

The vehicle data acquisition software employs multiple interface methods, including CAN bus and UART serial interfaces, to enable real-time collection and remote transmission of monitored parameters. Simultaneously, the software periodically sends remote data query frames compliant with the CAN 2.0B protocol, receives and parses data frames from various acquisition controllers, and updates corresponding monitoring data based on the unique ID of each sensor. This enables real-time display and storage of data from all sensor channels. The software continuously monitors measurement data transmitted over the CAN bus network and reads data from the RS232 serial interface. After analyzing and processing raw data, it displays and stores the harvester's position information, travel parameters, and operational status in real time via a graphical interface. Simultaneously, it performs fault logic judgments, providing real-time alerts on the current fault status of each critical working component.

Table 5 Identification results of combine working state alarm

Operating state	Number of test samples	Accurate number of alerts	Accuracy rate/%
Standby mode	200	198	99.0
Only the feeding auger is rotating during harvest	200	197	98.5
High-position harvesting of header in short-time and stable state	200	194	97.0
High-position harvesting of header in long-time and stable state	200	191	95.5
Feeding auger high speed	200	193	96.5
Total	1000	973	97.3

Figure 10 shows the software interface of the combine harvester's onboard terminal. Built using the LabVIEW graphical development environment, this interface follows a design philosophy emphasizing data visualization and functional modularity. By synchronizing with CAN bus data from the onboard terminal, the interface displays and records real-time operational parameters of the agricultural machinery's core modules during field operations. These modules include: machine status display, task positioning display, task quality and evaluation results display, and engine data display. Data refreshes at 1 s intervals, and users can switch between target functional modules by clicking the corresponding buttons. Operational fluidity meets software interaction standards, facilitating rapid information retrieval during field operations.

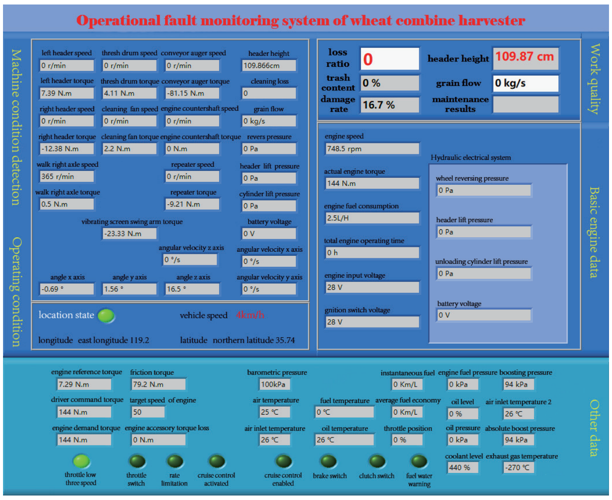

left header speed 0 r/min
thresh drum speed 0 r/min
conveyor auger speed 0 r/min
header height 109.866cm
left header torque 7.39 N.m
thresh drum torque 4.11 N.m
conveyor auger torque -81.15 N.m
cleaning loss 0
right header speed 0 r/min
cleaning fan speed 0 r/min
engine countershaft speed 0 r/min
grain flow 0 kg/s
right header torque -12.38 N.m
cleaning fan torque 2.2 N.m
engine countershaft torque 0 N.m
revers pressure 0 Pa
walk right axle speed 365 r/min
repeater speed 0 r/min
header lift pressure 0 Pa
walk right axle torque 0.5 N.m
repeater torque -9.21 N.m
cylinder lift pressure 0 Pa
vibrating screen swing arm torque -23.33 N.m
battery voltage 0 V
angular velocity z axis 0 °/s
angular velocity x axis 0 °/s
angle x axis -0.69 °
angle y axis 1.56 °
angle z axis 16.5 °
angular velocity y axis 0 °/s
location state
vehicle speed 4km/h
longitude east longitude 119.2
latitude northern latitude 35.74

loss ratio 0
header height 109.87 cm
trash content 0 %
grain flow 0 kg/s
damage rate 16.7 %
maintenance results

engine speed 748.5 rpm
actual engine torque 144 N.m
engine fuel consumption 2.5L/H
total engine operating time 0 h
engine input voltage 28 V
gnition switch voltage 28 V
wheel reversing pressure 0 Pa
header lift pressure 0 Pa
unloading cylinder lift pressure 0 Pa
battery voltage 0 V

engine reference torque 7.29 N.m
friction torque 79.2 N.m
barometric pressure 100kPa
instantaneous fuel 0 Km/L
engine fuel pressure 0 kPa
boosting pressure 94 kPa
driver command torque 144 N.m
target speed of engine 50
air temperature 25 ℃
fuel temperature 0 ℃
average fuel economy 0 Km/L
oil level 0 %
air inlet temperature 2 26 ℃
engine demand torque 144 N.m
engine accessory torque loss 0 N.m
air inlet temperature 26 ℃
oil temperature 26 ℃
throttle position 0 %
oil pressure 0 kPa
absolute boost pressure 94 kPa
coolant level 440 %
exhaust gas temperature -270 ℃

Figure 10 Upper computer interface of vehicle terminal

All parameters displayed in the critical parameter area of Figure 10 fall within normal ranges, indicating that the harvester operates stably under full load. If parameters exceed normal limits, the indicator light immediately changes color from green to red, triggering a visual alert. The blank list above will then display the fault code, fault description, and occurrence time.

According to the design requirements and functional specifications of the remote monitoring system, the cloud platform handles both real-time data acquisition from harvester monitoring and alarm and control signals. Through parallel computing and data mining analysis of collected data, it diagnoses potential harvester malfunctions. If a fault is detected, the system displays the fault information on the local screen and transmits it via the communication network to the remote monitoring cloud, enabling real-time remote monitoring of the harvester's operational status.

Traditional agricultural machinery remote monitoring platforms primarily rely on data storage and basic query functions, exhibiting inherent limitations such as low data processing efficiency, inability to support large-scale device connectivity, and insufficient data value extraction capabilities. To address these issues, this system innovatively constructs a cloud-based data processing architecture, enabling real-time processing and analysis of harvester operational data. The edge computing module integrated into the vehicle terminal performs preprocessing on massive collected data, including data cleansing and removal of outliers caused by sensor failures, while retaining key parameters related to malfunctions. Non-critical operational data is stored locally for only three days. This architecture supports concurrent connections from over 100 000 harvesters, achieving sub-second data processing to empower precision agricultural decision-making.

5 Conclusions and future work

This study establishes a comprehensive operational monitoring and fault warning system for wheat combine harvesters based on CAN bus technology, achieving multi-dimensional innovation upon existing techniques:

Overcoming the limitations of traditional single-parameter monitoring, it integrates engine fuel consumption, rotational speeds of seven key working components, torque of critical parts, and grain carry-over losses to form a comprehensive, end-to-end monitoring system for operational status and quality.

For mainstream domestic models such as the Lovol GE60, a modular sensor installation scheme was designed. Strain-gauge torque sensors were affixed to drive shafts and header shafts, while pulley-type torque sensors were employed for the chopping roller and conveyor fan. This approach avoids extensive modifications to the machine's transmission structure, significantly reducing installation costs and resolving compatibility challenges faced by foreign systems.

Employing multi-parameter correlation analysis, we developed fault warning algorithms featuring characteristic recognition and dynamic thresholds. This prevents misdiagnosis or missed detection caused by isolated parameter monitoring. Operators can adjust operations based on real-time feedback, preempting breakdowns, reducing harvest losses, and enhancing efficiency, directly boosting farmers' yields and income.

The integration of an on-board terminal developed using LabVIEW with a cloud-based monitoring platform enables real-time local display and remote data storage. This provides maintenance guidance during faults, reducing manual inspection and maintenance costs.

This system holds potential for future extension to other agricultural machinery, such as tractors and seed drills, tailored to the harvesting characteristics of crops like maize and rice. Deep integration with IoT and artificial intelligence technologies could further enhance fault identification and human-machine interaction efficiency. In summary, the monitoring system developed in this study achieves the collection, reception, and storage of multi-source sensor data onboard machinery. It improves the reliability and real-time capability of field data acquisition, providing technical support for advancing agricultural mechanization towards intelligent and precision-based operations.

Acknowledgments

This work was financially supported by the Subproject of the National Key Research and Development Program of China (Grant No. 2022YFD20015053).

[References]

[1] Zhao C J. Current situations and prospects of smart agriculture. Journal of South China Agricultural University, 2021; 42(6): 1–7.

[2] Jiang L, Wang G Q, Xu B Y, Husnain N, Wang Q. Intelligent systems for combine harvesters: a comprehensive review of technologies and trends. IEEE Access, 2025; 13: 189074–189095.

[3] Du X W, Ji J T, Jin X, Li C, Yang X L. Research on divider losses with high-speed photography for foxtail millet harvesting. Future Generation Computer Systems, 2018; 88: 55–60.

[4] Sinha B B, Dhanalakshmi R. Recent advancements and challenges of Internet of Things in smart agriculture: A survey. Future Generation Computer Systems, 2022; 126: 169–184.

[5] Xu H, Wu T, Liu Q T, Zhang Z X, Gan X T, Lian X L. Investigation of the trajectory of expelled billets from the chopping rollers of a sugarcane harvester. Sugar Tech, 2020; 22(5): 896–910.

[6] Debauche O, Mahmoudi S, Manneback P, Lebeau F. Cloud and distributed architectures for data management in agriculture 4. 0: Review and future trends. Journal of King Saud University - Computer and Information Sciences, 2022; 34(9): 7494–7514.

[7] Liu P, Jin C Q, Yang T X, et al. Design and experiment of multi parameter adjustable and measurable cleaning system. Transactions of the Chinese Society for Agricultural Machinery, 2020; 51(S2): 191–201. (in Chinese)

[8] Liu Y B, Li Y M, Dong Y H, Huang M S, Zhang T, Cheng J H. Development of a variable-diameter threshing drum for rice combine harvester using MBD-DEM coupling simulation. Computers and Electronics in Agriculture, 2022; 196: 106859.

[9] Kurita H, Iida M, Cho W, Suguri M. Rice autonomous harvesting: Operation framework. Journal of Field Robotics, 2017; 34(6): 1084–1099.

[10] Yang L L, Tian W Z, Xu Y Y, Wu C C. Predicting fuel consumption of grain combine harvesters based on random forest. Transactions of the CSAE, 2021; 37(9): 275–281.

[11] Zhang Y W, Yin Y X, Meng Z J, Chen D, Qin W C, Wang Q, et al. Development and testing of a grain combine harvester throughput monitoring system. Computers and Electronics in Agriculture, 2022; 200: 107253.

[12] Paul K, Chatterjee S S, Pai P, Varshney A, Juikar S, Prasad V, et al. Viable smart sensors and their application in data driven agriculture. Computers and Electronics in Agriculture, 2022; 198: 107096.

[13] Li B, Liu Y L, Zhang H, Jiang Q. A knowledge-based system for intelligent control model of rice and wheat combine harvester. International Journal of Pattern Recognition and Artificial Intelligence, 2022; 36(3): 2259008.

[14] Sharma K, Shivandu S K. Integrating artificial intelligence and internet of things (IoT) for enhanced crop monitoring and management in precision agriculture. Sensors International, 2024; 5: 100292.

[15] Wang H Y, Lao L Y, Zhang H L, Tang Z, Qian P F, He Q. Structural fault detection and diagnosis for combine harvesters: a critical review. Sensors, 2025; 25(13): 3851.

[16] Yılmaz D, Gökduman M E. Development of a measurement system for noise and vibration of combine harvester. Int J Agric & Biol Eng, 2020; 13(6): 104–108.

[17] Qiu Z M, Shi G X, Zhao B, Jin X, Zhou L M. Combine harvester remote monitoring system based on multi-source information fusion. Computers and Electronics in Agriculture, 2022; 194: 106771.

[18] Chen J, Wang S Q, Lian Y. Design and test of header parameter keys electric control adjusting device for rice and wheat combined harvester. Transactions of the Chinese Society of Agricultural Engineering (Transactions of the CSAE), 2018; 34(16): 19–26.

[19] Li R C, Cheng Y, Xu J K, Li Y C, Ding X K, Zhao S. Research on online monitoring system of hydraulic actuator of combine harvester. Processes, 2022; 10(1): 35.

[20] Chen J B, Zhou H L, Hu H Y, Song Y, Gifu D, Li Y Z, et al. Research on agricultural monitoring system based on convolutional neural network. Future Generation Computer Systems, 2018; 88: 271–278.

[21] Almufareh M F, Humayun M, Ahmad Z, Khan A. An intelligent LoRaWAN-based IoT device for monitoring and control solutions in smart farming through anomaly detection integrated with unsupervised machine learning. IEEE Access, 2024; 12: 119072–119086.

[22] Wu Y H, Li X Y, Mao E R, Du Y F, Yang F. Design and development of monitoring device for corn grain cleaning loss based on piezoelectric effect. Computers and Electronics in Agriculture, 2020; 179: 105793.

[23] Yin Y X, Zhang Y W, Meng Z J, Du C, Qin W C, Guo S X. Design and experiment of multi-information collection system for grain combine harvesters. IFAC-Papers Online, 2018; 51(17): 855–860.

[24] Bala A, Rashid R Z J A, Ismail I, Oliva D, Muhammad N, Sait S M, et al. Artificial intelligence and edge computing for machine maintenance: a review. Artificial Intelligence Review, 2024; 57(5): 119.

[25] Xiang W, Liu S, Li H K, Cao S, Zhang K L, Yang C. Fault diagnosis of gearbox based on refined topology and spatio-temporal graph convolutional network. IEEE Sensors Journal, 2024; 24(2): 1866–1879.